Modeling the overproduction of ribosomes when antibacterial drugs act on cells

Arijit Maitra* and Ken A. Dill†
Laufer Center for Physical and Quantitative Biology and Departments of Chemistry and Physics Stony Brook University, Stony Brook, USA, NY 11794.
(Dated: August 14, 2015)

Bacteria that are subjected to ribosome inhibiting antibiotic drugs show an interesting behavior: although adding drugs slows down cell growth, it also paradoxically increases the cell's concentration of ribosomes. We combine a prior nonlinear model of the energy-biomass balance in undrugged *E. coli* cells (*Maitra and Dill, PNAS 2015*) with Michaelis-Menten binding of drugs that inactivate ribosomes. Predictions are in good agreement with experiments on ribosomal concentrations and synthesis rates vs. drug concentrations and growth rates. The model indicates that the cell overproduces ribosomes in order to maintain an essentially constant ratio of active ribosomes to nonribosomal proteins, a key controller of cell behavior. The model also shows that drugged cells tend to maintain patterns of energy influx rates (glucose → ATP) that are the same as when the cells are undrugged. And, it predicts that adding drugs to slow-growing cells leads to a maximum point in the rate of ribosome synthesis. This type of modeling can provide insights into cellular driving forces that are difficult to measure.

1. INTRODUCTION

Drugs, such as chloramphenicol, act to reduce bacterial cell growth rates by inhibiting bacterial ribosomes, thereby reducing the cell's production of proteins. What actions does the cell evoke to counter the drug? On the one hand, there is often a good understanding of how the drug binds at its ribosomal site [1–3] and it is sometimes known how that binding interferes with protein elongation [4–7]. It is also sometimes known how drugs sensitize local networks to evoke adaptive responses [8–11]. On the other hand, there is usually less understanding of what global stresses the drug trigger, how it shifts the balances of energy and biomass, or of what homeostatic condition the cell might be trying to preserve.

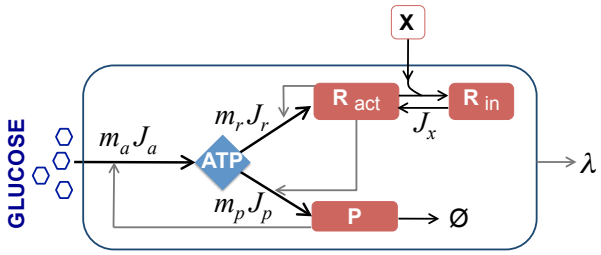

Figure 1: **Minimal kinetic model of *E. coli***. The model expresses the dynamical fluxes (arrows) and concentrations of active ribosomes (R_{act}), non-ribosomal proteins (P) and a lumped internal energy (ATP). Antibiotic inhibitor molecules are represented by X. X bind reversibly with active ribosomes. While in bound-form, R_{in}, the ribosomes are inactivated, and they do not translate proteins. P degrades with a rate constant γ. The cell grows exponentially with a specific growth rate of λ.

There are various approaches to cell-level modeling. One approach models the dynamics of the cell's networks of biochemical reactions [12–14]. Even in an organism as simple as a bacterium, there are very many interconnected web of reactions, making it complicated to model. Another approach has been Flux-Balance Analysis [15, 16], which gives solutions by linearizing the forces around some given homeostasis point. Here, however, we are interested in how those homeostasis points themselves are shifted by the drug. Homeostasis is a fundamentally nonlinear phenomenon, describing the cell's return to a stable state after a perturbation. Like the *Le Chatelier Principle* in physics [17], homeostasis describes a process resembling a marble rolling back to the bottom of a well after being pushed, like a well-bottom of an energy function. Here, we treat the nonlinearities and feedbacks that are needed to explore how the homeostasis balance is tipped by the drug. But to do this in a way that can give simple insights, we use a reduced ('minimalist') description of the bacterial cell [18]. We use this model to study the response of *E coli* to chloramphenicol.

Our goal here is a quantitative description of the energy-limited cell in the absence or presence of varying amounts of drug, in terms of the physico-chemical processes of the undrugged cell developed recently [18]. (By energy limited, we mean cells that are growth limited by a sugar source, such as glucose, rather than by amino acids, for example). Our minimal model expresses the dynamical concentrations and fluxes of three internal cell components – ribosomal protein, nonribosomal protein, and internal energy (lumped into a single category we call ATP), as a function of external sugar, such as glucose. We previously found that healthy *E. coli* under good growth conditions (speeds up to one duplication per hour) have achieved an evolutionary balance [18]. On the one hand, the cell invests energy and biomass in increasing its ribosome concentration because that increases the cell's growth speed. On the other hand, too much en-

*Electronic address: arijitmaitra1@gmail.com
†Electronic address: dill@laufercenter.org

ergy and biomass devoted to producing ribosomes leads to starving the cell's ability to take in food and convert it to ATP. In the present paper, we ask how drugging the cell affects its balance of energy and biomass.

2. A MINIMAL MODEL OF *E. COLI* IN THE PRESENCE OF DRUGS

We model the energy-limited growth of *E. coli* using three rate equations: for energy (ATP concentration, A) and ribosomal (R_{act}) and nonribosomal protein concentrations (P) as functions of time t [18]:

$$\frac{dA}{dt} = m_a J_a - m_r J_r - m_p J_p - \lambda A \tag{1}$$

$$\frac{dR_{act}}{dt} = J_r - J_x - \lambda R_{act} \tag{2}$$

$$\frac{dP}{dt} = J_p - (\gamma + \lambda)P \tag{3}$$

$$\rho = M_r(R_{act} + R_{in}) + M_p P, \tag{4}$$

where the fluxes are defined as:

$$J_r = k_r \cdot R_{act} \cdot f_r(A). \tag{5}$$

$$J_p = k_p \cdot R_{act} \cdot f_p(A) \tag{6}$$

$$J_a = k_a(G) \cdot P \tag{7}$$

Here, J_a is the rate of glucose conversion for ATP generation, J_p and J_r are the respective rates of synthesis of NRPs and ribosomes. k_r, k_p and $k_a(G)$ are the respective rate constants for ribosomal biogenesis, protein translation and energy generation. The units of rates and rate constants are 'mM per hour' and 'per hour' respectively. Our work is not the first to model the biomass balance in bacteria; see[19–25]. What is new here, we believe, is the coupling between the biomass and energy balance; also see [26].

The functional forms in Eqs. (5), (6), (7) reflect wild-type regulatory mechanisms that coordinate the syntheses of ribosomal and non-ribosomal proteins, which are complex [27, 28] and depend on the cell's energy status. To capture these dependencies, we adopt the undrugged cell functions [18]:

$$f_r(A) = \begin{cases} 0, & \text{if } A < D_r \\ f_r^{\infty} \cdot \left(1 - \frac{D_r}{A}\right), & \text{if } A \geq D_r \end{cases} \tag{8}$$

$$f_p(A) = f_p^{\infty} \cdot \frac{A}{D_p + A + D_{pp}A^2} \tag{9}$$

$$k_a(G) = k_a^{\infty} \cdot f_g(G) \cdot f_a(A) \tag{10}$$

$$f_g(G) = \frac{G^{1.5}}{G^{1.5} + {D_g}^{1.5}} \tag{11}$$

$$f_a(A) = \frac{D_a}{D_a + A}. \tag{12}$$

See S.I. for values of biophysical constants and parameters. In addition, here we consider the effects of drug X as shown in Fig. 1. X is an antibiotic drug that targets ribosomes. There is a broad class of natural and synthetic bacteriostatic antibiotics of this type, such as chloramphenicol, that target protein synthesis. The present model is intended as a general description of that class of drugs [3]. We assume X permeates *passively* from the extracellular medium into the cytosol through the cell membrane. We assume free drug concentrations outside and inside the cell are equal, a reasonable approximation for *E. coli* based on similar values of drug binding kinetics from invivo and invitro measurements, see Ref. [29, 30].

The binding of X to the ribosomes, which occurs with rate constant k_{+x}, halts peptide-chain elongation, as represented by the following dynamics:

$$\frac{dR_{in}}{dt} = k_{+x} \cdot x \cdot R_{act} - k_{-x} \cdot R_{in} - \lambda R_{in} \tag{13}$$

$$J_x = k_{+x} \cdot x \cdot R_{act} - k_{-x} \cdot R_{in}. \tag{14}$$

Here, x is the extracellular concentration of drugs. R_{in} is the concentration of ribosomes that have been *inactivated* by binding to the drug, and R_{act}, as noted above, is the intracellular concentration of *active* ribosomes. So, $R_{act} + R_{in}$ is the total concentration of ribosomes in the cell. J_x is the overall rate at which ribosomes become inactivated since $(k_{+x} \cdot x \cdot R_{act})$ is the rate of binding to the drug and $(k_{-x} \cdot R_{in})$ is the rate of unbinding.

A key quantity in the present model is the fraction of ribosomes that are active $\alpha(x)$, for a given drug concentration x. We assume steady state, so we set $dR_{in}/dt = 0$ in Eq. (13). We also assume that the rate constant for drug-ribosome unbinding is much faster than dilution, $k_{-x} \gg \lambda$. So, we get:

$$\frac{R_{act}}{R_{in}} = \frac{\lambda + k_{-x}}{k_{+x}x} \tag{15}$$

$$\Rightarrow \alpha(x) = \frac{R_{act}}{R_{act} + R_{in}} = \frac{1}{1 + (k_{+x}/k_{-x})x}. \tag{16}$$

For the equilibrium dissociation constant of chloramphenical, we use $(k_{-x}/k_{+x}) \equiv K_d \sim 3\mu M$ [29]. $\alpha = 1$ represents the situation of no drug. Increasing drug concentration decreases α towards zero.

The fraction of all proteins (by mass) that are active ribosomes is

$$\phi_{ac} \equiv \frac{M_r R_{act}}{M_r(R_{act} + R_{in}) + M_p P} = \alpha \phi_{tot}. \tag{17}$$

And, the fraction of all proteins that are all ribosomes (active plus inactive) is:

$$\phi_{tot} \equiv \frac{M_r(R_{act} + R_{in})}{M_r(R_{act} + R_{in}) + M_p P} = \frac{\lambda + \gamma}{\lambda + \gamma + \alpha k_p' f_p}. \tag{18}$$

The last equality in Eq. 18 expresses how the ribosomal content of the cell depends on its growth rate λ and other properties. Further, the rate of ribosome synthesis, $J_{fr} \equiv M_r J_r/\rho$, in units of g of ribosomal protein per g of total protein per hour can be computed as (see S.I.):

$$J_{fr} \equiv M_r J_r/\rho = \lambda \phi_{tot}. \tag{19}$$

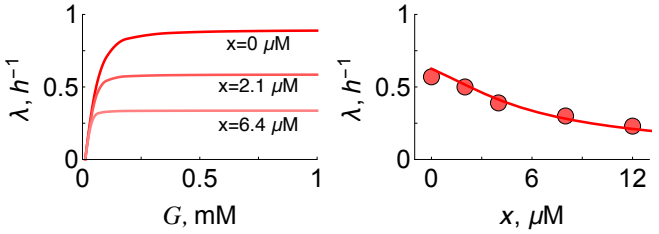

Figure 2: ***E. coli* physiological correlations.** (A) Growth rate vs. extracellular glucose concentration from simulation for antibiotic (chloramphenicol) concentrations of 0, 2.1 and 6.4 μM. (B) Dependence of growth rate, λ, on antibiotic concentration, x. Line is the numerical solution of the ODE model, with $G = 0.08$ mM, red. Red solid circles are experimental data [10, 32] of *E. coli* grown on glucose+M63.

Under growth conditions in the absence of drugs, $\alpha = 1$, and $f_p = f_p^\infty$ [18] the rate of ribosome synthesis is given as, using Eq. (18) and Eq. (19):

$$J_{fr} = \lambda \cdot \frac{\lambda + \gamma}{\lambda + \gamma + k_p' f_p^\infty}. \tag{20}$$

3. THE DRUGGED CELL OVERPRODUCES TOTAL RIBOSOMES TO MAINTAIN SUFFICIENTLY MANY ACTIVE RIBOSOMES

Here we describe the model predictions. We solve ODEs (1)-(14) under steady-state conditions for different concentrations of glucose and antibiotic drug. Fig. 2(A) shows that the model predicts Monod-like behavior [31] of growth rate vs. glucose concentration under different drug concentrations. As expected, the model predicts that increasing drug leads to diminishing maximum-growth rates.

Fig. 3 shows that the model is consistent with experiments indicating how added drug stimulates total ribosome production even as it reduces the cell's growth rate [10, 33]. The black line in Fig. 3 shows that, for undrugged cells, ribosomes become upshifted relative to other protein biomass with increasing cellular growth rate. The red line (and data points) show that added drug does two things: increases the ribosomal fraction while simultaneously reducing the growth rate.

What is the cell 'trying to achieve' under the burden of the drug? Fig. 4 gives insights; it shows that the cell maintains an essentially constant mass ratio, $R_{act}/(R_{act} + P)$, of active ribosomes to *useful proteins* (all proteins except inactive ribosomes). This is the basic quantity that controls the growth of the undrugged cell. That is, the cell overproduces total ribosomes so as to achieve sufficient active ribosomes in light of the increasing numbers of inactive ribosomes that result from increasing drug. To our knowledge, this ratio has not been measured experimentally.

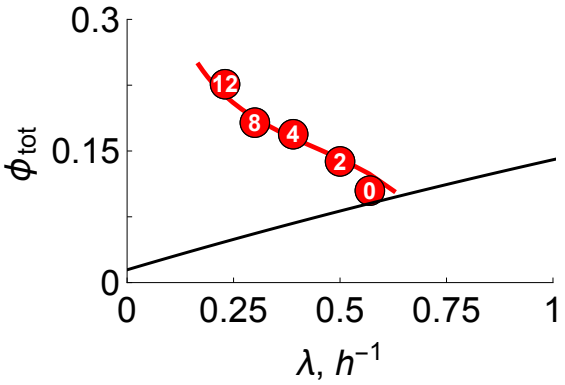

Figure 3: ***E. coli* ribosomal protein fraction vs growth rates.** Red line is the numerical solution of the ODE model, with glucose concentration $G = 0.08$ mM and antibiotic concentration $x = 0 - 15\mu$M. Circles are experimental data [10, 32] of *E. coli* grown on glucose+M63 at different dosage of chloramphenicol marked in μM. Black line is theory, Eq. (18) with $f_p = f_p^\infty = 0.7$, $k_p' = 9.65$ h^{-1}, $\gamma = 0.1$ h^{-1}, and $\alpha = 1$, absence of drugs.

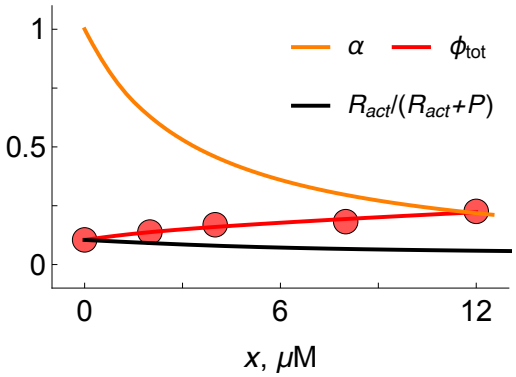

Figure 4: **Effect of ribosomal inhibitors on cellular homeostasis.** Solid circles are experimental data of ribosomal protein fraction ϕ_{tot} [10, 32] of *E. coli* grown on glucose+M63. Lines are numerical solutions of the ODE model, with $G = 0.08$ mM. Red line, total ribosomal protein fraction, $\phi_{tot} = M_r[R_{act} + R_{in}]/[M_r(R_{act} + R_{in}) + M_p P]$, at different dosage of chloramphenicol, x. Black line, $M_r R_{act}/(M_r R_{act} + M_p P)$ by mass. Orange, α, active fraction of ribosome independent of G and dependent hyperbolically on chloramphenicol concentration; see Eq. (16).

4. THE DRUG SHIFTS THE PRODUCTION RATE OF RIBOSOMES. BUT, IT HAS LITTLE EFFECT ON ENERGY FLOW FROM GLUCOSE TO ATP.

Fig. 5 illuminates the point from the perspective of total production rates of ribosomes. Fig. 5 shows $J_{fr} = \lambda \cdot \phi_{tot}(\lambda)$, the relation between rate production of total ribosomes and growth rate.

First, focus on the black line in Fig. 5. According

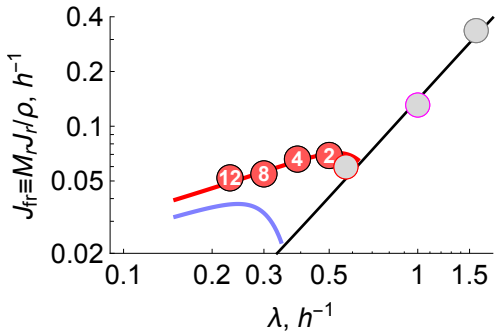

Figure 5: **Effect of ribosomal inhibitors on ribosomal activity.** The symbols show the rate of ribosomal synthesis $J_{fr} = M_r J_r/\rho$ vs. specific growth rate of *E. coli* converted from experimental $\phi - k$ data. Chloramphenicol concentrations (μM) marked inside the circles. Nutrients: M63+gluc (red) at T=37 C from Scott et al. [10, 32]. Gray filled circles are experimental data [10, 32] in the absence of drugs. Blue line; ODE model prediction at constant $G = 0.04$ mM and chloromaphenicol varied between $x = 0 - 15\mu$M. The black line is theory, Eq. (20), in the absence of drugs with $f_p = f_p^\infty = 0.7$, $\gamma = 0.1$ h^{-1}, $k_p' = 9.65$ h^{-1}. Also see S.I. Fig. S1.

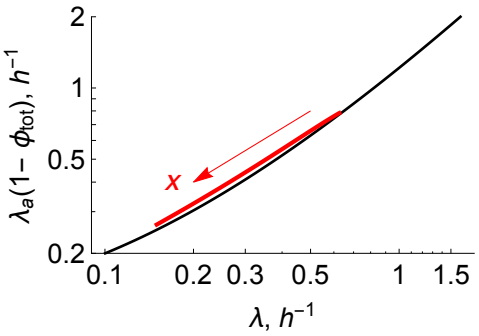

Figure 6: **Effect of ribosomal inhibitors on rate of energy metabolism.** Predictions of rate of energy metabolism vs. growth rate λ from ODE model under variation of glucose, $G = 0 - 1$ mM and no-drugs (black line). Prediction at $G = 0.04$ mM (red line) under variation of drugs from $x = 0 \to 15\mu$M shown by the arrow. Increase in drug concentration reduces both rates of growth and energy generation.

to the model, under no-drugs the ribosomal production rate should scale as the square of the growth rate, $J_{fr} \sim \lambda \cdot \lambda/(k_p' f_p^\infty) \propto \lambda^2$, since $\phi_{tot} \propto \lambda$. Fig. 5 shows a log-log plot. The black line shows the square-law prediction for undrugged cells. The data points shown in gray lay along this black line, indicating that the model predicts well the ribosomal production rates of undrugged cells growing at different speeds.

Next, focus on the red points in Fig. 5. The datapoints, containing the circled numbers 2 - 12 μM, show the effects of increasing amounts of drug at fixed nutrients. Following the red line toward the left, which describes increasing drug concentrations, shows how the drug reduces the growth rate while it also reduces the rate of total ribosome production. The experiments are from ref. [10]; also see SI.

Finally, the blue line on Fig. 5 makes an interesting prediction, for which there are no experiments yet as far as we know. The blue line represents cell growth under low nutrients, $0 < \lambda \lesssim 0.8$ h^{-1}. The blue line has curvature. Adding small amounts of drug increases the total ribosome production rates; adding much more drug leads to reduced rates of ribosome production because of its bigger effect on reducing the cell's growth rate.

Fig. 6 shows the prediction of $\lambda_a(1-\phi)$, which is a measure of flux of energy flow from glucose to ATP, $m_a k_a(G) \cdot P$. Fig. 6 shows that the drugged cell is maintaining this energy-flux correlation with growth rate at undrugged-cell levels, even at different levels of drug. As far as we know, there are no experiments that bear on this prediction.

5. DISCUSSION

We have shown here that this simple model is consistent with measured ribosomal concentrations vs. growth rate and drug concentrations. We would welcome additional experiments. Current experiments on drugged and undrugged bacteria are run on different food sources and in different media. Deeper tests of our model could come from studies that fix the types of nutrient and media, and vary only the food concentrations. In addition, a key variable here is λ_a, the cell's conversion efficiency of sugar to internal energy, such as ATP. It would be also valuable to have measurements of: glucose and oxygen uptake rates, ATP production rates ($m_a J_a$), ATP concentrations, and ribosome production rates (J_r), key glycolytic, TCA cycle, and fermentation enzyme concentrations as a function of external glucose and antibiotic concentrations.

Somewhat different models are those of Elf et al [34] and Deris et al [35], who consider bistabilities of cells resulting either from membrane properties or drug resistance. Other models focus on mechanisms of microscopic control of ribosome synthesis, such as the "stringent response", a negative feedback mechanism triggered when some of cell's excess usable energetic molecules are converted to unusable ppGpp as response to endogenous limitations of aminoacids [21, 28, 36]. Because of its simplicity, the present treatment could be extended to explore other factors that are of interest, such as cellular geometry (surface-volume considerations), multi-drug effects [37], or drug-dependent cellular multistabilities that lead to antibiotic resistance and persistence [34, 35].

6. CONCLUSIONS

Here, we model the balance of energy, ribosomes and nonribosomal proteins in *E. coli* cells in the presence

of chloramphenicol, an antibiotic drug. We suppose that chloramphenicol binds to ribosomes and inactivates them, in a Michaelis-Menten fashion. We combine this binding-induced inactivation with a three-component dynamical model of *E. coli's* energy, ribosomal and nonribosomal protein biomass as a function of growth rates, previously validated against experiments on undrugged bacteria. The present model gives quantitative predictions for how the cell's growth rate decreases with drug, and how the total ribosomal fraction of protein increases with drug. The main value of the model is not so much in fitting data as in giving deeper mechanistic insights into what the bacterium is 'trying to achieve' under increasing drug perturbations. We find that while drugging the cell causes dramatically lowered concentrations of active ribosomes, it also stimulates more total ribosome production, in an apparent effort to maintain a constant value of the balance of active ribosome to nonribosomal protein, a key quantity the cell uses to toggle between growth and self-protection.

Acknowledgement We appreciate support from the Laufer Center at Stony Brook University.

[1] J. Poehlsgaard and S. Douthwaite, Nature reviews. Microbiology **3**, 870 (2005), ISSN 1740-1526.
[2] T. Tenson and A. Mankin, Molecular microbiology **59**, 1664 (2006), ISSN 0950-382X.
[3] D. N. Wilson, Nature reviews. Microbiology **12**, 35 (2014), ISSN 1740-1534.
[4] C. Kurland and O. Maaloe, J Mol Biol **4**, 193 (1962).
[5] R. Coffman, T. Norris, and A. Koch, J Mol Biol. **60**, 1 (1971).
[6] D. Drainas, D. Kalpaxis, and C. Coutsogeorgopoulos, European J. Biochemistry **164**, 53 (1987).
[7] T. Siibak, L. Peil, L. Xiong, A. Mankin, J. Remme, and T. Tenson, Antimicrobial Agents and Chemotherapy **53**, 563 (2009), ISSN 00664804.
[8] C. Tamae, A. Liu, K. Kim, D. Sitz, J. Hong, E. Becket, A. Bui, P. Solaimani, K. P. Tran, H. Yang, et al., Journal of Bacteriology **190**, 5981 (2008), ISSN 00219193.
[9] M. A. Kohanski, D. J. Dwyer, and J. J. Collins, Nature reviews. Microbiology **8**, 423 (2010), ISSN 1740-1534.
[10] M. Scott, C. Gunderson, E. M. Mateescu, Z. Zhang, and T. Hwa, Science **330**, 1099 (2010).
[11] P. Nonejuie, M. Burkart, K. Pogliano, and J. Pogliano, Proceedings of the National Academy of Sciences of the United States of America **110**, 16169 (2013), ISSN 1091-6490.
[12] H. Kitano, Nat. Rev. Molec. Cell. Biol. **7**, 6511 (2006).
[13] M. Domach, S. Leung, R. Cahn, G. Cocks, and M. Shuler, Biotechnol. Bioeng. **26**, 203 (1984).
[14] C. Chassagnole, N. Noisommit-Rizzi, J. W. Schmid, K. Mauch, and M. Reuss, Biotechnology and Bioengineering **79**, 53 (2002), ISSN 00063592.
[15] J. D. Orth, I. Thiele, and B. O. Palsson, Nature biotechnology **28**, 245 (2010), ISSN 1546-1696.
[16] J. Edwards and B. Palsson, Proc. Natl. Acad. Sci. USA **97**, 5528 (2000).
[17] K. Dill and S. Bromberg, *Molecular Driving Forces: Statistical Thermodynamics in Chemistry and Biology* (Garland Science, 2003).
[18] A. Maitra and K. A. Dill, Proc. Natl. Acad. Sci. USA. **112**, 406 (2015).
[19] CN. Hinshelwood, J. Chem. Soc. pp. 745–755 (1952).
[20] H. Bremer and P. Dennis, *Modulation of chemical composition and other parameters of the cell by growth rate. In Escherichia coli and Salmonella., FC Neidhardt, ed* (American Society for Microbiology Press, Washington DC, 1996).
[21] M. Scott, S. Klumpp, E. Mateescu, and T. Hwa, Mol. Syst. Biol. **10**, 747 (2014).
[22] AG Marr, Microbiol. Rev. **55**, 316 (1991).
[23] D. Molenaar, R. van Berlo, D. de Ridder, and B. Teusink, Mol. Syst. Biol. **5**, 323 (2009).
[24] A. Zaslaver, S. Kaplan, A. Bren, A. Jinich, A. Mayo, E. Dekel, U. Alon, and S. Itzkovitz, PLoS Comput. Biol. **5**, e1000545 (2009).
[25] E. Bosdriesz, D. Molenaar, B. Teusink, and F. J. Bruggeman, FEBS Journal **282**, 2029 (2015), ISSN 1742-4658.
[26] A. Y. Weisse, D. A. Oyarzún, V. Danos, and P. S. Swain, Proceedings of the National Academy of Sciences USA **112**, 1038 (2015).
[27] G. B. M Nomura, RL Gourse, Annu. Rev. Biochem. **53**, 75 (1984).
[28] JJ Lemke, P Sanchez-Vazquez, HL Burgos, G Hedberg, W Ross, RL Gourse , Proc. Natl. Acad. Sci. USA. **108**, 5712 (2011).
[29] RJ. Harvey, AL. Koch, Antimicrob Agent Chemotherapy **18**, 323 (1980).
[30] O. Lewinson, J. Adler, G. J. Poelarends, P. Mazurkiewicz, A. J. M. Driessen, and E. Bibi, PNAS **100**, 1667 (2003).
[31] A. L. Koch, Journal of theoretical biology **98**, 401 (1982), ISSN 0022-5193.
[32] To get ϕ, the (rRNA/protein) ratio from Ref. [10] is scaled by a factor of 0.46 [20].
[33] P. Dennis, Journal of Molecular Biology **108**, 535 (1976).
[34] J. Elf, K. Nilsson, T. Tenson, and M. Ehrenberg, Phys. Rev. Lett. **97**, 258104 (2006).
[35] J. B. Deris, M. Kim, Z. Zhang, H. Okano, R. Hermsen, A. Groisman, and T. Hwa, Science (New York, N.Y.) **342**, 1237435 (2013), ISSN 1095-9203.
[36] B. P. English, V. Hauryliuk, A. Sanamrad, S. Tankov, N. H. Dekker, and J. Elf, Proceedings of the National Academy of Sciences of the United States of America **108**, E365 (2011), ISSN 1091-6490.
[37] T. Bollenbach, S. Quan, R. Chait, and R. Kishony, Cell **139**, 707 (2009), ISSN 1097-4172.

Supporting Information

Modeling the overproduction of ribosomes when antibacterial drugs act on cells

Arijit Maitra and Ken A. Dill
Laufer Center for Physical and Quantitative Biology and Departments of Chemistry and Physics
Stony Brook University, Stony Brook, USA, NY 11794.

1. RATE OF RIBOSOME CREATION

Here, we derive an expression for the rate of total ribosome production. Ribsomal inhibitors such as chloramphenicol reduce the cell's growth rate by reducing the active fraction of ribosomes. Adding Eq. (2) and Eq. (13) and setting the sum to zero gives

$$\lambda(\alpha) = \alpha k_r f_r(A), \tag{S1}$$

showing how the cell's growth rate is reduced with α, the ribosomal inactivation fraction in Eq. 16.

Here, we express the rate of ribosome synthesis, J_{fr}, in units of g of ribosomal protein per g of total protein, to get the points on Fig. 5 as computed from experimental data $\phi_{tot} - \lambda$:

$$J_r = R_{act} \cdot k_r f_r \text{ ; from Eq. (5)} \tag{S2a}$$
$$= \frac{R_{act}}{R_{act} + R_{in}} \cdot k_r f_r \cdot (R_{act} + R_{in}) \tag{S2b}$$
$$= \alpha \cdot k_r f_r \cdot (R_{act} + R_{in}) \text{ ; using Eq. (16)} \tag{S2c}$$
$$= \lambda \cdot (R_{act} + R_{in}) \text{ ; using Eq. (S1)} \tag{S2d}$$
$$\Rightarrow J_{fr} = \frac{M_r J_r}{\rho} \tag{S2e}$$
$$= \lambda \cdot \frac{M_r(R_{act} + R_{in})}{M_r(R_{act} + R_{in}) + M_p P} \tag{S2f}$$
via Eqs. (S2d) and (4)
$$= \lambda \phi_{tot} \tag{S2g}$$

Under growth conditions without antibiotics, the flux for ribosomal synthesis is:

$$J_{fr} = \lambda \frac{\lambda + \gamma}{\lambda + \gamma + k'_p f_p^{\infty}}. \tag{S3}$$

obtained from substituting Eq. (18) with $\alpha = 1$, $f_p = f_p^{\infty}$ into Eq. (S2g).

2. ENERGY BALANCE

Next, we look at the energy balance. At steady state, Eqs. (1), (2), (3) are set to zero, leading to the expression,

$$\lambda_a = \frac{(\lambda + \gamma)(\lambda + \alpha \lambda_p f_p)}{\alpha \lambda_p f_p} \tag{S4}$$

In addition, we now show how our model leads to the linear dependence of ribosomal content on growth rate described by Scott et al. [10]. We derive another expression for ϕ_{tot} from Eqs. (18) and (S4) by eliminating $\alpha k'_p f_p$:

$$\phi_{tot}[\lambda; \lambda_a(G)] = \frac{\lambda_a(G) - \gamma - \lambda}{\lambda_a(G) - \gamma + \lambda \epsilon_{rp}} \text{ where } \epsilon_{rp} = \frac{\epsilon_p - \epsilon_r}{\epsilon_r} \tag{S5}$$

Setting $\epsilon_{rp} \sim 0$ and $\gamma \sim 0$ gives $\phi_{tot}(\lambda) \sim 1 - \lambda/\lambda_a(G)$, giving the linear relationship of Scott et al. [10].

Table S1: Structural, Rate and Bioenergetic Constants.

Physical constants	Symbol	Value
Protein density	ρ	0.25 g cm^{-3}
Molec. wt. of ribosomal proteins (RP) per ribosome	M_r	7336 aa × 110 g/mol/aa = 806960 g mol^{-1}
Molec. wt. of a non-ribosomal protein (NRP)	M_p	325 aa × 110 g/mol/aa = 35750 g mol^{-1}
Molecules of ATP produced per glucose molecule	m_a	30
Molecules ATP consumed to create one ribosome	m_r	(7336 aa × 6) + (4566 nu × 10) ∼ 89700
Molecules of ATP consumed to create one NRP	m_p	325 aa × 6 = 1950
Rate of NRP elongation per ribosome, 20 aa/s	k_p'	20 × 3600 (aa/h)/7336 aa ∼ 10 aa/h/(RP aa)
Non-ribosomal protein degradation rate	γ	0.1 NRP per total NRP per h

Derived constants	Symbol	Value
Max no. of protein molecules translated per hr per ribosome (capacity)	k_p	$M_r k_p'/M_p$ = 215 h^{-1}
NRP translation rate per ribosome scaled by pathway efficiencies	λ_p	$(\varepsilon_r/\varepsilon_p)k_p'$ ∼ 5 h^{-1}
Max no. of ribosomes synthesized per hr per ribosome (= λ_p)	k_r	5 h^{-1}
Ribosomal pathway efficiency, g of RPs synthesized per mol ATP	ε_r	M_r/m_r ∼ 9 g mol^{-1}
Protein pathway efficiency, g of NRPs per mol ATP	ε_p	M_p/m_p ∼ 18 g mol^{-1}
Relative pathway efficiency between P– and R– pathways	ε_{rp}	$(\varepsilon_p - \varepsilon_r)/\varepsilon_r$ ∼ 1

Table S2: Parameters of *E. coli* ODE numerical model obtained from fit of the model to data.

ODE model Parameters	Symbol	Value
Affinity constant between nonribosomal proteins and glucose for glucose transport	D_g	0.07 mM
Number of glucose molecules metabolized to ATP per hr per protein molecule	k_a^∞	120 h^{-1}
Affinity constant between proteins and ATP for ATP generation	D_a	4.0 mM
ATP concentration threshold for ribosome synthesis	D_r	0.18 mM
Max fraction of ribosomes translating RPs	f_r^∞	0.2
Max fraction of ribosomes translating NRPs	f_p^∞	0.7

Table S3: Interaction parameters of *E. coli* and Chloramphenicol.

ODE model Parameters	Symbol	Value
Regulatory parameter of f_p	D_p	0.02 mM
Regulatory parameter of f_p	D_{pp}	1/15 mM^{-1}
Rate constant of chloramphenicol molecules to bind with a ribosome	k_{+x}	9 h^{-1} μM^{-1}
Ribosome-drug unbinding rate constant	k_{-x}	30 h^{-1}

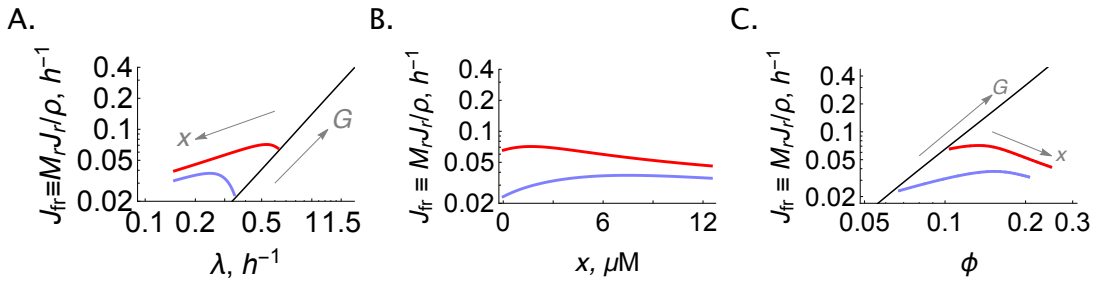

Figure S1: **Effect of ribosomal inhibitors on ribosomal activity.** (A) The black line is theory, Eq. (S3), in the absence of drugs with $f_p = f_p^\infty = 0.7$, $\gamma = 0.1$ h^{-1}, $k_p' = 9.65$ h^{-1}. Solutions of ODE cell model at G=0.04 mM (blue) and 0.08 mM (red), respectively, under increasing chloramphenicol concentrations, $x = 0 - 15\mu$M, shown by arrow. Black dashed line is maximal ribosomal flux possible from the cell model across different glucose concentrations. (B) Ribosomal activity vs. chloramphenicol concentration from ODE model at G=0.04 mM (blue) and 0.08 mM (red). (C) Ribosomal activity vs. ribosomal protein fraction from ODE model at G=0.04 mM (blue) and 0.08 mM (red).